

Gluon skewed generalized parton distributions of proton from a light-front Hamiltonian approach

Pengxiang Zhang^{a,b}, Yiping Liu^{b,c}, Siqi Xu^{b,c,d}, Chandan Mondal^{b,c,*}, Xingbo Zhao^{b,c}, James P. Vary^d,
(BLFQ Collaboration)

^aLanzhou University, Lanzhou, Gansu, 730000, China

^bInstitute of Modern Physics, Chinese Academy of Sciences, Lanzhou, Gansu, 730000, China

^cSchool of Nuclear Physics, University of Chinese Academy of Sciences, Beijing, 100049, China

^dDepartment of Physics and Astronomy, Iowa State University, Ames, IA 50011, USA

Abstract

We calculate all leading-twist gluon generalized parton distributions (GPDs) inside the proton at nonzero skewness using the basis light-front quantization framework. The proton's light-front wave functions are derived from a light-front quantized Hamiltonian incorporating Quantum Chromodynamics inputs. Our results show that the qualitative behaviors of the GPDs are consistent with those from other theoretical calculations. Additionally, we analyze the GPDs in the boost-invariant longitudinal coordinate, $\sigma = \frac{1}{2}b^-P^+$, which serves as the Fourier conjugate of the skewness. The GPDs in σ -space exhibit diffraction patterns, reminiscent of optical wave diffraction.

Keywords: GPDs, Gluons, Proton, Light-front quantization

1. Introduction

The proton, a bound state of quarks and gluon held together by the strong interaction described by quantum chromodynamics (QCD), is a central focus in nuclear and particle physics. Understanding its structure in terms of QCD's fundamental degrees of freedom is a major challenge. Over the past two decades, extensive experimental and theoretical efforts (see Ref. [1] and the references therein) have been dedicated to studying generalized parton distributions (GPDs), which capture the three-dimensional (3D) spatial structure of the proton.

Precise knowledge of GPDs is essential for analyzing and interpreting exclusive scattering processes, such as deeply virtual Compton scattering (DVCS) [2, 3], deeply virtual meson production (DVMP) [4–6], neutrino/electroweak meson production [7, 8] single diffractive hard exclusive processes (SDHEPs) [9–11], timelike Compton scattering (TCS) [12], wide-angle Compton scattering (WACS) [13, 14], and double DVCS [15]. Experimental collaborations worldwide, including Hall A [16, 17], CLAS [18–20] at Jefferson Lab (JLab), ZEUS [21, 22], H1 [23, 24], HERMES [25–27] at DESY, and COMPASS [28] at CERN,

etc., have made significant strides in investigating GPDs. GPDs provide crucial insights into the spatial distribution, spin, and orbital motion of partons inside the proton. Consequently, precise determination of proton GPDs is a primary objective for upcoming facilities like the Electron-Ion Colliders (EICs) [29–35], the Large Hadron-Electron Collider (LHeC) [36, 37], and the 12 GeV upgrade at JLab [38–40].

GPDs depend on the longitudinal momentum fraction (x) carried by the partons, the longitudinal momentum transfer (ξ) known as skewness, and the square of the total momentum transfer (t). In the forward limit, where $t = 0$ and $\xi = 0$, GPDs reduce to ordinary parton distribution functions (PDFs), which are accessible in deep inelastic scattering (DIS) experiments. The Mellin moments of GPDs correspond to form factors, and the Fourier transform of GPDs at zero skewness with respect to transverse momentum transfer yields impact parameter-dependent parton distributions, revealing how partons with specific longitudinal momentum are distributed in transverse position space [41, 42]. These distributions, unlike GPDs in momentum space, have a probabilistic interpretation and adhere to certain positivity conditions [43]. For nonzero skewness, GPDs can also be expressed in longitudinal position space via Fourier transformation with respect to the skewness variable ξ [44–51].

From a theoretical standpoint, various nonperturbative techniques have been employed to explore quark GPDs, often taking a more phenomenological approach [52–59].

*Corresponding author

Email addresses: zhangpx2021@lzu.edu.cn (Pengxiang Zhang), liuyiping@impcas.ac.cn (Yiping Liu), xsq234@impcas.ac.cn (Siqi Xu), mondal@impcas.ac.cn (Chandan Mondal), xbzhao@impcas.ac.cn (Xingbo Zhao), jvary@iastate.edu (James P. Vary)

Promising methods for obtaining GPDs include Euclidean lattice QCD [60–72]. While the study of gluon GPDs has not been as extensive as that of quark GPDs, recent research has increasingly focused on both chiral even and chiral odd gluon GPDs, particularly using light-cone spectator models [73–75], basis light-front quantization (BLFQ) [76, 77], and light-front holography [78, 79], double distribution representation [6], and holographic string-based approach [80, 81] to explore these leading-twist phenomena.

In this work, we explore all the leading-twist gluon GPDs of the proton at nonzero skewness using the non-perturbative framework, known as BLFQ [82–90]. While BLFQ has been previously applied to study gluon GPDs at zero skewness [76, 77], it is crucial to investigate GPDs at nonzero skewness, as experiments typically probe at $\xi \neq 0$. Within the BLFQ framework, an effective light-front Hamiltonian is used to determine the mass eigenstates and light-front wave functions (LFWFs), extending beyond the valence three-quark Fock sector ($|qqq\rangle$) to include the proton Fock sector with one dynamical gluon ($|qqqg\rangle$) [90–92]. We consider the QCD interaction applicable to both Fock sectors [93], supplemented by model confining potentials acting in both the transverse and longitudinal directions [84]. The resulting LFWFs have been successfully employed to study various proton properties, including electromagnetic form factors, radii, PDFs, GPDs, TMDs, and spin and orbital angular momentum [90–92]. In this study, we extend our investigations to examine gluon GPDs at nonzero skewness.

2. Proton LFWFs with a dynamical gluon

The LFWFs of the proton are obtained from the light-front¹ Hamiltonian by solving the eigenvalue equation: $H_{\text{LF}}|\Psi\rangle = M^2|\Psi\rangle$, where $H_{\text{LF}} = P^+P^- - \vec{P}_\perp^2$ represents the Hamiltonian of the proton with P^- being the light-front Hamiltonian, P^+ the longitudinal momentum, \vec{P}_\perp the transverse momentum, and M is the invariant mass of the system. At constant light-front time $x^+ = x^0 + x^3$, the proton state is expressed using various Fock sectors:

$$|\Psi\rangle = \psi_{qqq} |qqq\rangle + \psi_{qqqg} |qqqg\rangle + \dots, \quad (1)$$

where $\psi(\dots)$ represents the LFWFs corresponding to each Fock state $|\dots\rangle$. For practical computation, it is necessary to truncate the Fock space expansion to a finite number of dimensions. At the model scale, we describe the proton through the LFWFs for the valence quarks, denoted as ψ_{uud} , as well as configurations incorporating three quarks and an additional dynamical gluon, represented by ψ_{uudg} . We employ a light-front Hamiltonian, $P^- = P_0^- + P_1^-$,

where P_0^- represents the light-front QCD Hamiltonian corresponding to the $|qqq\rangle$ and $|qqqg\rangle$ Fock states of the proton, and P_1^- signifies a model Hamiltonian for the confining interaction potential [90].

In the light-front gauge $A^+ = 0$, the light-front QCD Hamiltonian with a dynamical gluon is given by [89, 90],

$$P_0^- = \int dx^- d^2x^\perp \left\{ \frac{1}{2} \bar{\psi} \gamma^+ \frac{m_0^2 + (i\partial^\perp)^2}{i\partial^+} \psi + \frac{1}{2} A_a^i [m_g^2 + (i\partial^\perp)^2] A_a^i + g_c \bar{\psi} \gamma_\mu T^a A_a^\mu \psi + \frac{1}{2} g_c^2 \bar{\psi} \gamma^+ T^a \psi \frac{1}{(i\partial^+)^2} \bar{\psi} \gamma^+ T^a \psi \right\}. \quad (2)$$

The first two terms in Eq. (2) represent the kinetic energy of quarks and gluons, with bare masses m_0 for quarks and m_g for gluons. Here, ψ denotes the quark field, and A_a^i represents the gluon field. The Dirac matrices are denoted by γ^μ , and T is the generator of the SU(3) gauge group in color space. Although gluons are massless in standard QCD, our model introduces a phenomenological gluon mass to better capture low-energy phenomena as discussed in Ref. [90]. The third and fourth terms in Eq. (2) describe quark-gluon interactions through vertex and instantaneous gluon interactions, governed by the coupling constant g_c . Following Fock-sector dependent renormalization [94–96], a mass counter-term (δm_q) is added to adjust the quark mass within the leading Fock sector to its renormalized value, $m_q = m_0 - \delta m_q$. Additionally, the model permits an independent quark mass m_f in vertex interactions as suggested in Refs. [97, 98].

The confining potential within the leading Fock sector, which includes both transverse and longitudinal components, is given by [89, 90],

$$P_1^- P^+ = \frac{\kappa^4}{2} \sum_{i \neq j} \left\{ \vec{r}_{ij\perp}^2 - \frac{\partial_{x_i}(x_i x_j \partial_{x_j})}{(m_i + m_j)^2} \right\}, \quad (3)$$

where $\vec{r}_{ij\perp}$ quantifies the transverse distance between quarks, and κ represents the strength of the confinement. For the $|qqqg\rangle$ Fock state, our model does not include an explicit confinement term. Instead, it relies on the effective mass of the gluon and the selected basis to account for confinement effects at the scale of the model.

In the BLFQ approach [82], we use two-dimensional harmonic oscillator (2D-HO) basis functions $\Phi_{nm}(p_\perp; b)$ with the energy scale b , defined by radial (n) and angular (m) quantum numbers, to describe transverse degrees of freedom [84]. For longitudinal motion, plane-wave basis functions are employed within a box of length $2L$, with anti-periodic (fermions) or periodic (bosons) boundary conditions. Longitudinal momentum is given by $p^+ = \frac{\pi}{L} k$, where k is a half-integer (integer) for fermions (bosons). We omit the zero mode for bosons. Each single-particle basis state is characterized by four quantum numbers $|\alpha_i\rangle = |k_i, n_i, m_i, \lambda_i\rangle$, where λ denotes the light-front helicity. Multi-body basis states are constructed as the direct

¹We adopt the light-front convention for the four-vector $v = (v^+, v^-, v^\perp)$, where $v^\pm = v^0 \pm v^3$ and $v^\perp = (v^1, v^2)$.

product of single-particle states, $|\alpha\rangle = \otimes_i |\alpha_i\rangle$ and we ensure a total color singlet configuration. All Fock-sector basis states share the same total angular momentum projection M_j , satisfying the condition $\sum_i (\lambda_i + m_i) = M_j$.

We impose cutoffs, \mathcal{K} and \mathcal{N}_{\max} , to constrain the basis in the longitudinal and transverse directions. The total longitudinal momentum is given by $\mathcal{K} = \sum_i k_i$, with each parton's momentum fraction $x_i = k_i/\mathcal{K}$. The transverse energy cutoff, $\mathcal{N}_{\max} \geq \sum_i (2n_i + |m_i| + 1)$, sets the range for 2D-HO states and determines the infrared (IR) and ultraviolet (UV) cutoffs, approximated as $\lambda_{\text{IR}} \approx b/\sqrt{\mathcal{N}_{\max}}$ and $\lambda_{\text{UV}} \approx b\sqrt{\mathcal{N}_{\max}}$, respectively [83].

Diagonalizing the light-front Hamiltonian matrix provides the mass-squared spectra, M^2 , and the LFWFs in momentum space:

$$\Psi_{N, \{x_i, \vec{p}_{i\perp}, \lambda_i\}}^{M_j} = \sum_{\{n_i m_i\}} \psi_N^{M_j}(\{\alpha_i\}) \prod_{i=1}^N \Phi_{n_i m_i}(\vec{p}_{i\perp}, b), \quad (4)$$

where $\psi_{N=3}^{M_j}(\alpha_i)$ and $\psi_{N=4}^{M_j}(\alpha_i)$ correspond to the $|uud\rangle$ and $|uudg\rangle$ sectors, respectively. In this paper, all calculations are performed with $N_{\max} = 9$ and $K = 16.5$. The effective Hamiltonian parameters are chosen to reproduce the proton mass and fit the flavor form factors [90]. The LFWFs, suitable for a low-resolution probe at $\mu_0^2 \sim 0.24 \pm 0.01 \text{ GeV}^2$ [90], have been successfully applied to compute a wide range of proton observables, such as electromagnetic form factors, radii, PDFs, GPDs, TMDs, and spin and orbital angular momentum, etc., [90–92].

Table 1: The nucleon's GPDs depending on the polarization of the nucleon (N) and the gluon (g) with $\bar{E}_T = 2\tilde{H}_T + E_T$. The symbols U, L, and T represent the nucleon polarizations, i.e., unpolarized, longitudinally polarized, and transversely polarized, respectively and U, Circular, and Linear represent the gluon polarizations, i.e., unpolarized, circularly polarized, and linearly polarized, respectively.

N/g	U	Circular	Linear
U	H		\bar{E}_T
L		\tilde{H}	\tilde{E}_T
T	E	\tilde{E}	H_T, \tilde{H}_T

3. Gluon generalized parton distributions

At leading twist, the proton has eight gluon GPDs: four chirally even (H , E , \tilde{H} , and \tilde{E}) and four chirally odd (H_T , E_T , \tilde{H}_T , and \tilde{E}_T). These GPDs relate to the polarization of the proton and gluons, as summarized in Table 1, and are defined through the off-forward matrix elements of the

bilocal gluon tensor operator between proton states [99]:

$$F_{\Lambda, \Lambda'}^g = \frac{1}{\bar{P}^+} \int \frac{dz^-}{2\pi} e^{ix\bar{P}^+z^-} \times \langle P', \Lambda' | F^{+i} \left(-\frac{z}{2} \right) F^{+i} \left(\frac{z}{2} \right) | P, \Lambda \rangle \Big|_{\substack{z^+=0 \\ z^-=0}} \quad (5)$$

$$= \frac{1}{2\bar{P}^+} \bar{u}(P', \Lambda') \left[H^g \gamma^+ + E^g \frac{i\sigma^{+\alpha}(-\Delta_\alpha)}{2M} \right] u(P, \Lambda),$$

$$\tilde{F}_{\Lambda, \Lambda'}^g = \frac{-i}{\bar{P}^+} \int \frac{dz^-}{2\pi} e^{ix\bar{P}^+z^-} \times \langle P', \Lambda' | F^{+i} \left(-\frac{z}{2} \right) \tilde{F}^{+i} \left(\frac{z}{2} \right) | P, \Lambda \rangle \Big|_{\substack{z^+=0 \\ z^-=0}} \quad (6)$$

$$= \frac{1}{2\bar{P}^+} \bar{u}(P', \Lambda') \left[\tilde{H}^g \gamma^+ \gamma_5 + \tilde{E}^g \frac{\gamma_5(-\Delta_\alpha)}{2M} \right] u(P, \Lambda),$$

$$F_{T\Lambda, \Lambda'}^g = -\frac{1}{\bar{P}^+} \int \frac{dz^-}{2\pi} e^{ix\bar{P}^+z^-} \times \langle P', \Lambda' | \mathbf{S} F^{+i} \left(-\frac{z}{2} \right) F^{j+} \left(\frac{z}{2} \right) | P, \Lambda \rangle \Big|_{\substack{z^+=0 \\ z^-=0}} \quad (7)$$

$$= \frac{\mathbf{S}}{2\bar{P}^+} \frac{[\bar{P}, \Delta]^{+j}}{2M\bar{P}^+} \bar{u}(P', \Lambda') \left[i\sigma^{+i} H_T^g + \frac{[\gamma, \Delta]^{+i}}{2M} E_T^g \right. \\ \left. + \frac{[\bar{P}, \Delta]^{+i}}{M^2} \tilde{H}_T^g + \frac{[\gamma, \bar{P}]^{+i}}{M} \tilde{E}_T^g \right] u(P, \Lambda),$$

where $F^{+\mu}(x) = \partial^+ A^\mu(x)$ corresponds to the gluon field tensor in the light-cone gauge and the dual field strength is given by $\tilde{F}^{\alpha\beta}(x) = \frac{1}{2}\epsilon^{\alpha\beta\gamma\delta} F_{\gamma\delta}(x)$. \mathbf{S} stands for symmetrization of uncontracted Lorentz indices and removal of the trace. A summation over $i, j = 1, 2$ is implied. We use a compact notation $[a, b]^{+i} = a^+b^i - b^+a^i$. In the symmetric frame, the average momentum of proton $\bar{P} = \frac{1}{2}(P' + P)$, while momentum transfer $\Delta = (P' - P)$. The initial and final four momenta of the proton are then given by

$$P \equiv \left((1 + \xi)\bar{P}^+, \frac{M^2 + \Delta_\perp^2/4}{(1 + \xi)\bar{P}^+}, -\vec{\Delta}_\perp/2 \right), \quad (8)$$

$$P' \equiv \left((1 - \xi)\bar{P}^+, \frac{M^2 + \Delta_\perp^2/4}{(1 - \xi)\bar{P}^+}, \vec{\Delta}_\perp/2 \right). \quad (9)$$

Note that all the GPDs are functions of x , $\xi = -\Delta^+/2\bar{P}^+$, and $t = \Delta^2$. One can derive the following relation explicitly from Δ^-

$$-t = \frac{4\xi^2 M^2 + \Delta_\perp^2}{(1 - \xi^2)}. \quad (10)$$

In a reference frame where the momenta \vec{P}' and \vec{P} lie in the $x - z$ plane [52], we explicitly derive the relations for

the chiral-even GPDs as follows:

$$\begin{aligned}
H^g(x, \xi, t) &= \frac{1}{\sqrt{1-\xi^2}} F_{++}^g + \frac{2M\xi^2}{\sqrt{1-\xi^2}\Delta_{\perp 1}} F_{-+}^g, \\
E^g(x, \xi, t) &= \frac{2M\sqrt{1-\xi^2}}{\Delta_{\perp 1}} F_{-+}^g, \\
\tilde{H}^g(x, \xi, t) &= \frac{1}{\sqrt{1-\xi^2}} \tilde{F}_{++}^g + \frac{2M\xi}{\sqrt{1-\xi^2}\Delta_{\perp 1}} \tilde{F}_{-+}^g, \\
\tilde{E}^g(x, \xi, t) &= -\frac{2M\sqrt{1-\xi^2}}{\xi\Delta_{\perp 1}} \tilde{F}_{-+}^g,
\end{aligned} \tag{11}$$

where the proton helicity is denoted by $\Lambda = +(-)$, corresponding to $+1(-1)$, respectively. For the chiral-odd GPDs, we transform the matrix elements from the helicity basis to the transversity basis [50, 52] and decompose the gluon tensor operator into $\theta_1 = F^{+1}F^{1+} - F^{+2}F^{2+}$ and $\theta_2 = i(F^{+1}F^{2+} + F^{+2}F^{1+})$ [99]. In the transversity basis, we obtain

$$\begin{aligned}
H_T^g(x, \xi, t) &= -\frac{2M}{\sqrt{1-\xi^2}\Delta_{\perp 1}} F_{\uparrow\uparrow}^{g[\theta_1]} - \frac{4M^2\xi}{\sqrt{1-\xi^2}\Delta_{\perp 1}^2} F_{\downarrow\downarrow}^{g[\theta_1]}, \\
E_T^g(x, \xi, t) &= \frac{4M^2}{\sqrt{1-\xi^2}\Delta_{\perp 1}^2} \left(\xi F_{\downarrow\uparrow}^{g[\theta_1]} + F_{\uparrow\uparrow}^{g[\theta_2]} \right) \\
&\quad + \frac{8M^3}{\sqrt{1-\xi^2}\Delta_{\perp 1}^3} \left(F_{\uparrow\downarrow}^{g[\theta_2]} - F_{\uparrow\uparrow}^{g[\theta_1]} \right), \\
\tilde{H}_T^g(x, \xi, t) &= -\frac{4M^3\sqrt{1-\xi^2}}{\Delta_{\perp 1}^3} \left(F_{\uparrow\downarrow}^{g[\theta_2]} - F_{\uparrow\uparrow}^{g[\theta_1]} \right), \\
\tilde{E}_T^g(x, \xi, t) &= \frac{4M^2}{\sqrt{1-\xi^2}\Delta_{\perp 1}^2} \left(F_{\downarrow\uparrow}^{g[\theta_1]} + \xi F_{\uparrow\uparrow}^{g[\theta_2]} \right) \\
&\quad + \frac{8M^3\xi}{\sqrt{1-\xi^2}\Delta_{\perp 1}^3} \left(F_{\uparrow\downarrow}^{g[\theta_2]} - F_{\uparrow\uparrow}^{g[\theta_1]} \right),
\end{aligned} \tag{12}$$

where

$$\begin{aligned}
F_{\Lambda_T, \Lambda_T}^{g[\theta_i]} &= -\frac{1}{\bar{P}^+} \int \frac{dz^-}{2\pi} e^{ix\bar{P}^+z^-} \\
&\quad \times \langle P', \Lambda_T' | \theta_i | P, \Lambda_T \rangle \Big|_{z^\perp=0}, \tag{13}
\end{aligned}$$

with $\Lambda_T = \uparrow (\downarrow)$ being the transverse polarization of the proton polarized along the +ve \hat{x} (\downarrow) or -ve \hat{x} (\uparrow) direction. In overlap representation, $F_{\Lambda\Lambda'}^g$, $\tilde{F}_{\Lambda\Lambda'}^g$, and $F_{\Lambda_T\Lambda_T'}^{g[\theta_i]}$ are expressed in terms of the LFWFs as

$$\begin{aligned}
F_{\Lambda', \Lambda}^g &= \sum_{\{\lambda_i\}} \int [d\mathcal{X} d\mathcal{P}_\perp] \Psi_{4, \{x_i'', \vec{k}_{i\perp}'', \lambda_i\}}^{\Lambda'*} \Psi_{4, \{x_i', \vec{k}_{i\perp}', \lambda_i\}}^\Lambda, \\
\tilde{F}_{\Lambda', \Lambda}^g &= \sum_{\{\lambda_i\}} \int [d\mathcal{X} d\mathcal{P}_\perp] \lambda_1 \Psi_{4, \{x_i'', \vec{k}_{i\perp}'', \lambda_i\}}^{\Lambda'*} \Psi_{4, \{x_i', \vec{k}_{i\perp}', \lambda_i\}}^\Lambda,
\end{aligned} \tag{14}$$

$$\begin{aligned}
F_{\uparrow\uparrow}^{g[\theta_1]} &= \sum_{\{\lambda_i, \lambda_i'\}} \int [d\mathcal{X} d\mathcal{P}_\perp] \Psi_{4, \{x_i'', \vec{k}_{i\perp}'', \lambda_i'\}}^{-*} \Psi_{4, \{x_i', \vec{k}_{i\perp}', \lambda_i\}}^+ \\
&\quad \times \delta_{\lambda_1', -\lambda_1} \delta_{\lambda_{2,3,4}', \lambda_{2,3,4}}, \\
F_{\downarrow\downarrow}^{g[\theta_1]} &= \sum_{\{\lambda_i, \lambda_i'\}} \int [d\mathcal{X} d\mathcal{P}_\perp] \Psi_{4, \{x_i'', \vec{k}_{i\perp}'', \lambda_i'\}}^{+*} \Psi_{4, \{x_i', \vec{k}_{i\perp}', \lambda_i\}}^+ \\
&\quad \times \lambda_1' \delta_{\lambda_1', -\lambda_1} \delta_{\lambda_{2,3,4}', \lambda_{2,3,4}}, \\
F_{\uparrow\uparrow}^{g[\theta_2]} &= \sum_{\{\lambda_i, \lambda_i'\}} \int [d\mathcal{X} d\mathcal{P}_\perp] \Psi_{4, \{x_i'', \vec{k}_{i\perp}'', \lambda_i'\}}^{+*} \Psi_{4, \{x_i', \vec{k}_{i\perp}', \lambda_i\}}^+ \\
&\quad \times \delta_{\lambda_1', -\lambda_1} \delta_{\lambda_{2,3,4}', \lambda_{2,3,4}}, \\
F_{\downarrow\downarrow}^{g[\theta_2]} &= \sum_{\{\lambda_i, \lambda_i'\}} \int [d\mathcal{X} d\mathcal{P}_\perp] \Psi_{4, \{x_i'', \vec{k}_{i\perp}'', \lambda_i'\}}^{-*} \Psi_{4, \{x_i', \vec{k}_{i\perp}', \lambda_i\}}^+ \\
&\quad \times (-\lambda_1') \delta_{\lambda_1', -\lambda_1} \delta_{\lambda_{2,3,4}', \lambda_{2,3,4}},
\end{aligned} \tag{15}$$

where

$$\begin{aligned}
[d\mathcal{X} d\mathcal{P}_\perp]_n &= (\sqrt{1-\xi^2})^{2-n} \prod_{i=1}^n \left[\frac{dx_i d^2\vec{k}_{i\perp}}{16\pi^3} \right] \delta(x-x_1) \\
&\quad \times 16\pi^3 \delta \left(1 - \sum_{i=1}^3 x_i \right) \delta^2 \left(\sum_{i=1}^3 \vec{k}_{i\perp} \right), \tag{16}
\end{aligned}$$

and the light-front momenta are $x_1' = \frac{x_1+\xi}{1+\xi}$; $\vec{k}_{1\perp}' = \vec{k}_{1\perp} + (1-x')\frac{\vec{\Delta}_\perp}{2}$ for the initial gluon ($i=1$) and $x_i' = \frac{x_i}{1+\xi}$; $\vec{k}_{i\perp}' = \vec{k}_{i\perp} - x_i'\frac{\vec{\Delta}_\perp}{2}$ for the initial spectators ($i \neq 1$) and $x_1'' = \frac{x_1-\xi}{1-\xi}$; $\vec{k}_{1\perp}'' = \vec{k}_{1\perp} - (1-x'')\frac{\vec{\Delta}_\perp}{2}$ for the final gluon and $x_i'' = \frac{x_i}{1-\xi}$; $\vec{k}_{i\perp}'' = \vec{k}_{i\perp} + x_i''\frac{\vec{\Delta}_\perp}{2}$ for the final spectators and $\lambda_1(\lambda_1')$ designates the gluon helicity. Note that, in this work, we limit ourselves to the Dokshitzer-Gribov-Lipatov-Altarelli-Parisi (DGLAP) region, $\xi < x < 1$, where the number of partons in the initial and the final states remains conserved.

4. Numerical results and discussions

In our BLFQ approach, the use of a discretized plane-wave basis in the longitudinal direction results in discretized momentum fractions for the partons, $x_i = \frac{k_i}{\mathcal{K}}$, where k_i are half-integers for the quarks and integers for the gluon. Calculating GPDs at nonzero skewness involves overlapping LFWFs with different longitudinal momenta. We interpolate the longitudinal component of our LFWFs to obtain all leading-twist GPDs. These GPDs are related to physical quantities such as orbital angular momentum, axial and tensor charges, and are also connected to form factors and PDFs in specific kinematic limits [99]. In presenting our numerical results, we focus on the ξ -dependence of the gluon GPDs, as the other dependencies with vanishing skewness have been explored in previous studies [76, 77].

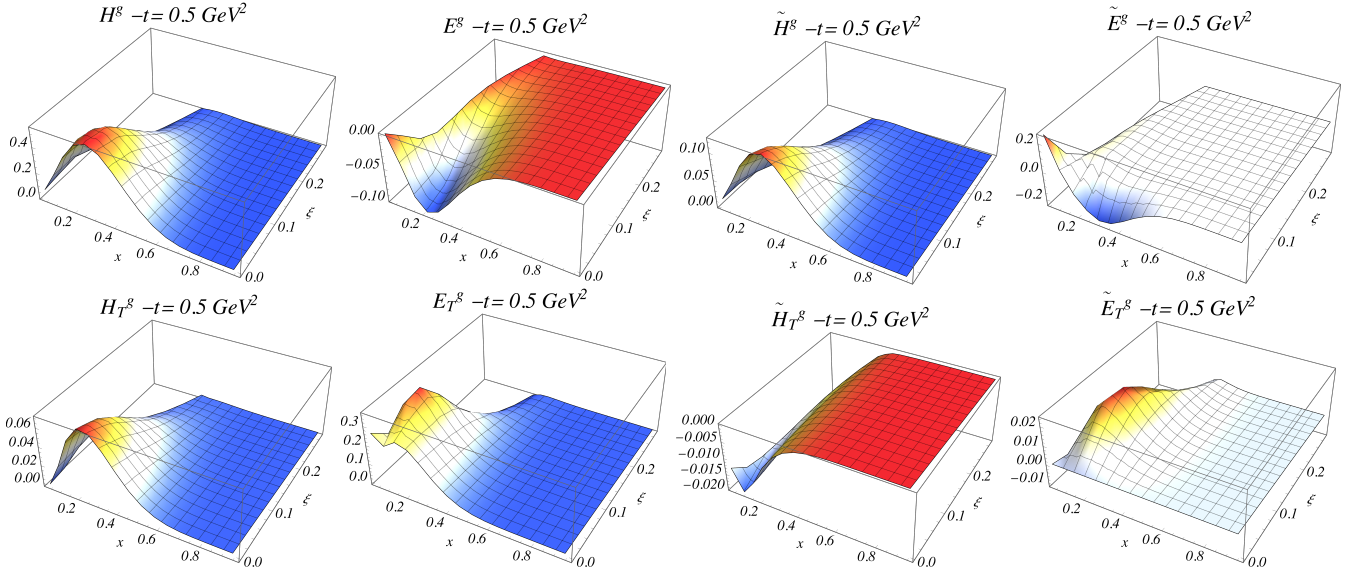


Figure 1: The gluon GPDs as functions of x and ξ for fixed $t = -0.5 \text{ GeV}^2$. The upper (lower) panel is for the chiral-even (odd) GPDs.

4.1. GPDs in momentum space

In Fig. 1 (upper panel), we present the gluon chiral-even GPDs as functions of x and ξ for a fixed value of $t = -0.5 \text{ GeV}^2$. The general features of these GPDs are similar, differing mainly by overall sign and scale, with the exception of \tilde{E}^g (discussed below). All GPDs peak at lower x (< 0.5), with peaks shifting to higher x and diminishing as the longitudinal momentum transfer increases. In the large x region, all GPDs eventually decay and become independent of ξ . Both H^g and \tilde{H}^g show positive peaks along ξ , while E^g shows negative peaks, with maximum values at $\xi = 0$. The peak of H^g is notably larger than those of E^g and \tilde{H}^g , which are comparable in magnitude. The GPD \tilde{E}^g behaves differently, crossing zero along x at small ξ . The forward limits of H^g and \tilde{H}^g correspond to spin-independent and spin-dependent gluon PDFs, respectively, as reported in Ref. [90]. In contrast, E^g and \tilde{E}^g have no forward limits and decouple in this regime [99].

When comparing our results with those from the light-cone spectator models [73, 78], a significant difference emerges. In our case, both H^g and \tilde{H}^g are positive definite, whereas the spectator models exhibit negative regions at small x and oscillatory behavior in x space. However, the qualitative behavior of E^g and \tilde{E}^g in Ref. [78] is consistent with our findings. Additionally, the overall behavior of our gluon GPDs is similar to those of quark GPDs in the proton [49, 51, 55, 100–103] and in the pion [104]. Notably, within our BLFQ approach, the gluon GPDs decrease more rapidly with increasing ξ compared to the quark GPDs [100].

All the chiral-odd GPDs, shown in Fig. 1 (lower panel), display similar qualitative behavior to the chiral-even GPDs, except for \tilde{E}_T^g . The GPD \tilde{E}_T^g vanishes at $\xi = 0$. It is an odd function under the transformation $\xi \rightarrow -\xi$ [99],

satisfying $\tilde{E}_T^g(x, -\xi, t) = -\tilde{E}_T^g(x, \xi, t)$. Except for \tilde{H}_T^g , all other chiral-odd GPDs show positive distributions. H_T^g and \tilde{H}_T^g peak at $\xi = 0$, while E_T^g and \tilde{E}_T^g have positive peaks along ξ , with extrema around $\xi \sim 0.1$ for $-t = 0.5 \text{ GeV}^2$. The peak shifts to larger x with increasing ξ . We observe that the signs and qualitative features of H_T^g and E_T^g in our BLFQ analysis are consistent with those obtained using the quark target model [105] and light-cone spectator model [74]. Additionally, in our study, \tilde{H}_T^g is distinctly non-zero, differing from those phenomenological model outcomes. A notable distribution emerges from combining two chiral-odd GPDs, $2\tilde{H}_T^g + E_T^g$, which offers insights into transverse spin and angular momentum contributions in specific limits [77, 106, 107]. All distributions show accessibility of the DGLAP region $x > \xi$, with the distribution width in x decreasing as ξ increases. The qualitative behavior of our gluon chiral-odd GPDs aligns with quark GPDs [50, 52, 100].

Figure 2 shows the gluon chiral-even (upper panel) and chiral-odd GPDs (lower panel), respectively, as functions of x and $-t$ for a fixed $\xi = 0.1$. The distributions peak when there is no transverse momentum transfer to the proton's final state and when the gluon carries less than 50% of the proton's longitudinal momentum. As momentum transfer increases, the peak shifts towards higher x values, while the magnitude decreases. In the large x region, all distributions eventually decay and become independent of $-t$, with a faster decay for the chiral-odd GPDs compared to the chiral-even GPDs. We also notice that E and E_T fall faster than H and H_T . We observe a bump in \tilde{E} at $-t \sim 2 \text{ GeV}^2$, occurring at a value of x where other GPDs nearly vanish. Notably, \tilde{H}_T has a sharp negative peak at $x \sim \xi$ and decays more rapidly with $-t$ than \tilde{E}_T . These characteristics are model and parton-independent, consistent with observations in quark distributions in various

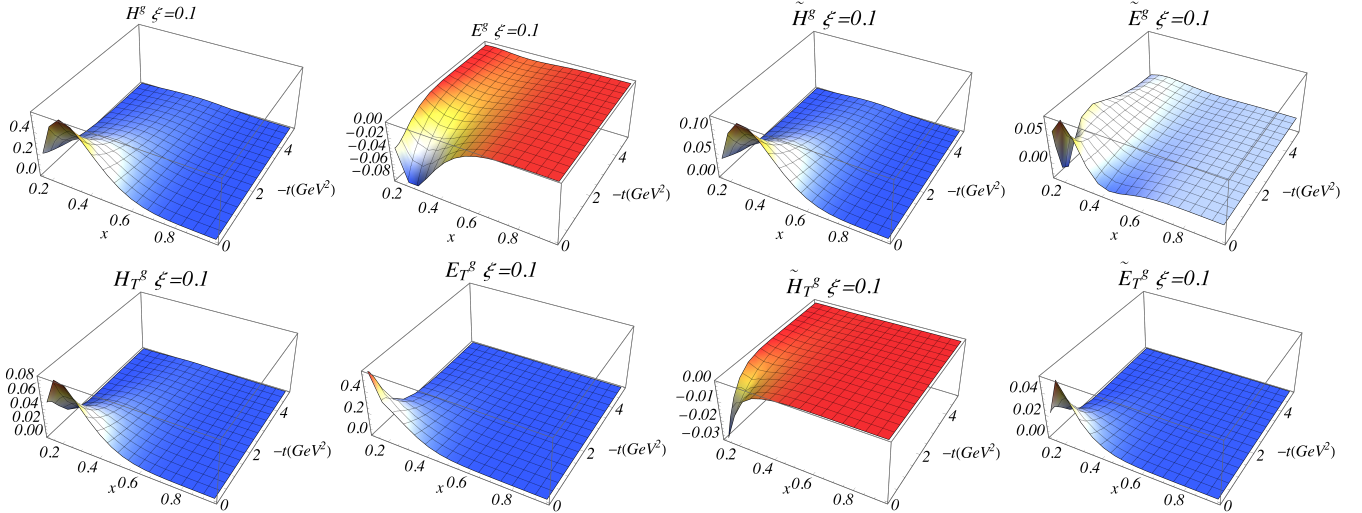


Figure 2: The gluon GPDs as functions of x and $-t$ for fixed $\xi = 0.1$. The upper (lower) panel is for the chiral-even (odd) GPDs.

QCD-inspired models [49–52, 55, 101–103] as well as in our BLFQ approach [100].

In the forward limit, GPDs reduce to PDFs, such as the unpolarized and helicity-dependent PDFs, with $H(x, 0, 0) = f_1(x)$ and $\tilde{H}(x, 0, 0) = g_1(x)$, respectively. Unlike the quark transversity PDF, $H_T(x, 0, 0) = h_1(x)$, a gluon transversity PDF does not exist for a spin- $\frac{1}{2}$ target, as gluon helicity flip requires targets with spin 1 or higher for angular momentum conservation. Studies on gluon PDFs, angular momentum, and generalized form factors corresponding to GPDs H , E , \tilde{H} , and $2\tilde{H}_T^q + E_T^q$ within our BLFQ approach are reported in Refs. [76, 77, 90].

4.2. GPDs in boost-invariant longitudinal space

The GPDs in transverse position space have been widely studied using various theoretical approaches, including the BLFQ framework at zero skewness. The transverse impact parameter \vec{b}_\perp is the Fourier conjugate to the variable $\vec{D}_\perp = \vec{\Delta}_\perp / (1 - \xi^2)$ [42, 43, 104, 108], which simplifies to $\vec{\Delta}_\perp$ at zero skewness. Similarly, the longitudinal momentum transfer ξP^+ is the Fourier conjugate to the longitudinal distance $\frac{1}{2}b^-$. Thus, ξ is conjugate to the boost-invariant longitudinal impact parameter $\sigma = \frac{1}{2}b^- P^+$. Fourier transforming the GPDs with respect to ξ provides distributions in boost-invariant longitudinal space σ , where the DVCS amplitude reveals a diffraction pattern [44, 45], akin to optical diffraction. This makes exploring GPDs in longitudinal impact parameter space particularly intriguing. The GPDs in this space are defined as follows:

$$\begin{aligned} f(x, \sigma, t) &= \int_0^{\xi_f} \frac{d\xi}{2\pi} e^{i\xi P^+ b^- / 2} G(x, \xi, t) \\ &= \int_0^{\xi_f} \frac{d\xi}{2\pi} e^{i\xi \sigma} G(x, \xi, t), \end{aligned} \quad (17)$$

where G stands for the GPDs. The upper integration limit, ξ_f , plays a role analogous to the slit width in diffraction, setting a key condition for the emergence of the diffraction pattern. Since we focus on the region $\xi < x < 1$, the upper limit is defined as $\xi_f = \min\{x, \xi_{\max}\}$. For a fixed value of $-t$, the maximum value of ξ is given by [109]

$$\xi_{\max} = \frac{1}{\left[1 + \frac{4M^2}{(-t)}\right]^{\frac{1}{2}}}. \quad (18)$$

Figure 3 presents our results for the modulus of the gluon's chiral-even (upper panel) and chiral-odd GPDs (lower panel), respectively in longitudinal position space for three different values of $x = \{0.2, 0.4, 0.6\}$ with a fixed $t = -1.0 \text{ GeV}^2$. The chosen value of $-t$ corresponds to $\xi_{\max} \approx 0.47$, setting the upper limit for the ξ integration in Eq. (17). Specifically, $\xi_f = 0.2$ and 0.4 for $x = 0.2$ and 0.4 , respectively, while for $x = 0.6$, the integration limit is $\xi_f = 0.47$ since $x > \xi_{\max}$ in this case.

Our results show oscillatory behavior similar to the diffraction pattern seen in a single-slit optical experiment, where the width of the principal maxima is inversely proportional to the slit width. In the Fourier transform described by Eq. (17), the finite range of ξ generates this diffraction pattern, with ξ_f acting as the slit width. However, not all functions with a finite range of ξ produce such a pattern; for example, $\tilde{E}^g(x, \sigma, t)$ and $\tilde{E}_T^g(x, \sigma, t)$ behave differently compared to the other GPDs.

A major feature appears as ξ_f increases, where the principal maxima narrow, with the first minima shifting inward. Similar patterns have been observed in DVCS amplitudes, coordinate-space parton densities, and Wigner distributions in various models [44–51, 104, 110–112]. Notably, gluon GPDs in longitudinal position space show different characteristics compared to quark GPDs. The diffraction pattern is prominent at small x for gluons but

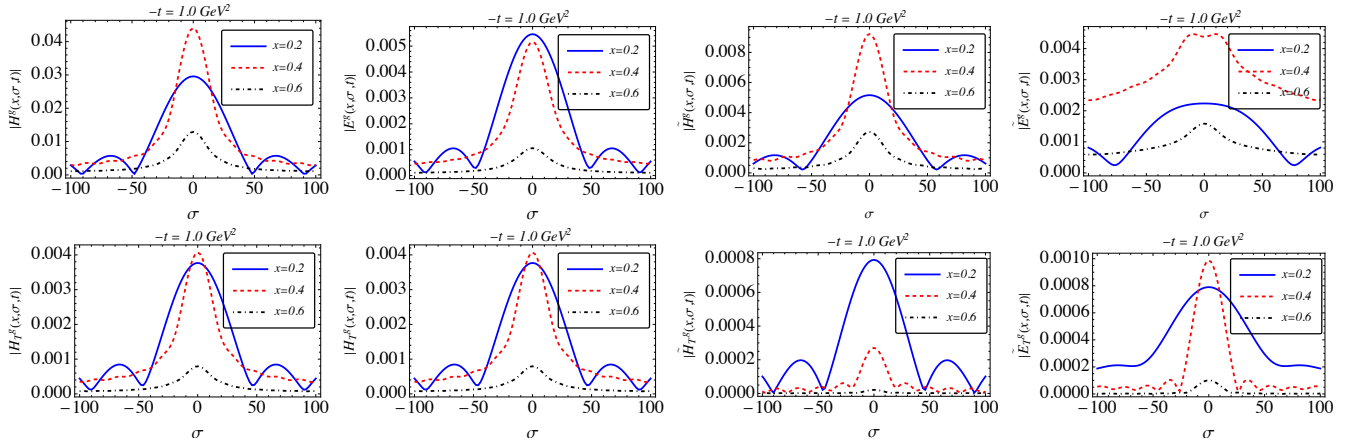


Figure 3: The gluon GPDs in boost-invariant longitudinal position space as functions of σ for $x = \{0.2, 0.4, 0.6\}$ and fixed $t = -1.0 \text{ GeV}^2$. The upper (lower) panel is for the chiral-even (odd) GPDs.

transitions into a single peak as x increases, while quark distributions retain the pattern even at large x . This difference arises from the more rapid decline of gluon GPDs with increasing ξ compared to quark GPDs [100]. Additionally, all distributions in boost-invariant longitudinal space show a long-distance tail, as noted in Refs. [110, 113]. We observe that gluon distributions exhibit longer tails compared to quark distributions [100].

5. Conclusions

The study of gluon skewness-dependent GPDs is of interest due to their connection with exclusive scattering cross sections, measurable in EIC and EicC experiments. Using BLFQ, a nonperturbative tool for solving many-body bound state problems in quantum field theory, we calculated all leading-twist, gluon skewed GPDs for the proton from its LFWFs. These wave functions were obtained from the eigenvectors of an effective QCD Hamiltonian, incorporating three-dimensional confinement and fundamental QCD interactions. We focused on the DGLAP region ($x > \xi$), where our BLFQ approach shows qualitative similarities with other phenomenological models. Interestingly, \tilde{H}_T^g is non-zero, unlike other models [73, 74, 105], and gluon GPDs decrease more rapidly with increasing ξ compared to quark GPDs [100].

The gluon GPDs in longitudinal impact-parameter space offer a unique view of the proton's structure. By performing a Fourier transform of the skewed GPDs with respect to ξ , we obtained the GPDs in boost-invariant longitudinal position space, $\sigma = \frac{1}{2}b^-P^+$. These gluon GPDs exhibit a diffraction pattern similar to that observed in single-slit optical experiments, where the central maxima's width is inversely proportional to the slit width, represented here by the finiteness of ξ_f . However, this pattern is influenced by the functional behavior of the GPDs as well. Notably, gluon GPDs in longitudinal position space

differ from quark GPDs, showing a prominent diffraction pattern at small x that transitions into a single peak as x increases, whereas quark distributions maintain the pattern even at large x . Additionally, gluon distributions exhibit longer tails compared to quark distributions [100]. A similar diffraction pattern has been observed in various observables, including the DVCS amplitude, parton density, and Wigner distributions in longitudinal position space.

We will extend our approach to include the $|qqq\bar{q}\bar{q}\rangle$ and $|qqqqg\rangle$ Fock sectors, enabling the evaluation of skewed GPDs in the ERBL region ($x < \xi$) and the study of sea-quark GPDs. This approach will also be applied to calculate higher-twist GPDs [114], with future work focusing on genuine contributions beyond the Wandzura-Wilczek approximation.

Acknowledgements

We thank Bolang Lin, Sreeraj Nair, Ziqi Zhang, Zhimin Zhu, and Zhi Hu for helpful discussions in the Institute of Modern Physics, University of Chinese Academy of Science. C. M. is also supported by new faculty start up funding by the Institute of Modern Physics, Chinese Academy of Sciences, Grant No. E129952YR0. X. Zhao is supported by new faculty startup funding by the Institute of Modern Physics, Chinese Academy of Sciences, by Key Research Program of Frontier Sciences, Chinese Academy of Sciences, Grant No. ZDBS-LY-7020, by the Foundation for Key Talents of Gansu Province, by the Central Funds Guiding the Local Science and Technology Development of Gansu Province, Grant No. 22ZY1QA006, by international partnership program of the Chinese Academy of Sciences, Grant No. 016GJHZ2022103FN, by National Key R&D Program of China, Grant No. 2023YFA1606903, by the Strategic Priority Research Program of the Chinese Academy of Sciences, Grant No. XDB34000000, and by the National Natural Science Foundation of China under

Grant No.12375143. J. P. V. is supported by the Department of Energy under Grant No. DE-SC0023692. A major portion of the computational resources were also provided by Sugon Advanced Computing Center.

References

- [1] S. Diehl, Experimental exploration of the 3D nucleon structure, *Prog. Part. Nucl. Phys.* 133 (2023) 104069. [doi:10.1016/j.pnpnp.2023.104069](#).
- [2] X.-D. Ji, Deeply virtual Compton scattering, *Phys. Rev. D* 55 (1997) 7114–7125. [arXiv:hep-ph/9609381](#), [doi:10.1103/PhysRevD.55.7114](#).
- [3] K. Goeke, M. V. Polyakov, M. Vanderhaeghen, Hard exclusive reactions and the structure of hadrons, *Prog. Part. Nucl. Phys.* 47 (2001) 401–515. [arXiv:hep-ph/0106012](#), [doi:10.1016/S0146-6410\(01\)00158-2](#).
- [4] S. V. Goloskokov, P. Kroll, The Role of the quark and gluon GPDs in hard vector-meson electroproduction, *Eur. Phys. J. C* 53 (2008) 367–384. [arXiv:0708.3569](#), [doi:10.1140/epjc/s10052-007-0466-5](#).
- [5] J. C. Collins, L. Frankfurt, M. Strikman, Factorization for hard exclusive electroproduction of mesons in QCD, *Phys. Rev. D* 56 (1997) 2982–3006. [arXiv:hep-ph/9611433](#), [doi:10.1103/PhysRevD.56.2982](#).
- [6] S. V. Goloskokov, Y.-P. Xie, X. Chen, Study of gluon GPDs in exclusive J/ψ production in electron-proton scattering, *Phys. Rev. D* 110 (7) (2024) 076029. [arXiv:2408.05800](#), [doi:10.1103/PhysRevD.110.076029](#).
- [7] B. Pire, L. Szymanowski, Exclusive neutrino production of a charmed vector meson and transversity gluon generalized parton distributions, *Phys. Rev. D* 96 (11) (2017) 114008. [arXiv:1711.04608](#), [doi:10.1103/PhysRevD.96.114008](#).
- [8] B. Pire, L. Szymanowski, J. Wagner, Charged current electroproduction of a charmed meson at an electron-ion collider, *Phys. Rev. D* 104 (9) (2021) 094002. [arXiv:2104.04944](#), [doi:10.1103/PhysRevD.104.094002](#).
- [9] J.-W. Qiu, Z. Yu, Single diffractive hard exclusive processes for the study of generalized parton distributions, *Phys. Rev. D* 107 (1) (2023) 014007. [arXiv:2210.07995](#), [doi:10.1103/PhysRevD.107.014007](#).
- [10] O. Grocholski, B. Pire, P. Sznajder, L. Szymanowski, J. Wagner, Phenomenology of diphoton photoproduction at next-to-leading order, *Phys. Rev. D* 105 (9) (2022) 094025. [arXiv:2204.00396](#), [doi:10.1103/PhysRevD.105.094025](#).
- [11] G. Duplanić, S. Nabeebaccus, K. Passek-Kumerički, B. Pire, L. Szymanowski, S. Wallon, Accessing chiral-even quark generalised parton distributions in the exclusive photoproduction of a $\gamma\pi^\pm$ pair with large invariant mass in both fixed-target and collider experiments, *JHEP* 03 (2023) 241. [arXiv:2212.00655](#), [doi:10.1007/JHEP03\(2023\)241](#).
- [12] E. R. Berger, M. Diehl, B. Pire, Time-like Compton scattering: Exclusive photoproduction of lepton pairs, *Eur. Phys. J. C* 23 (2002) 675–689. [arXiv:hep-ph/0110062](#), [doi:10.1007/s100520200917](#).
- [13] A. V. Radyushkin, Nonforward parton densities and soft mechanism for form-factors and wide angle Compton scattering in QCD, *Phys. Rev. D* 58 (1998) 114008. [arXiv:hep-ph/9803316](#), [doi:10.1103/PhysRevD.58.114008](#).
- [14] M. Diehl, T. Feldmann, R. Jakob, P. Kroll, Linking parton distributions to form-factors and Compton scattering, *Eur. Phys. J. C* 8 (1999) 409–434. [arXiv:hep-ph/9811253](#), [doi:10.1007/s100529901100](#).
- [15] K. Deja, V. Martinez-Fernandez, B. Pire, P. Sznajder, J. Wagner, Phenomenology of double deeply virtual Compton scattering in the era of new experiments, *Phys. Rev. D* 107 (9) (2023) 094035. [arXiv:2303.13668](#), [doi:10.1103/PhysRevD.107.094035](#).
- [16] C. Muñoz Camacho, et al., Scaling tests of the cross-section for deeply virtual compton scattering, *Phys. Rev. Lett.* 97 (2006) 262002. [arXiv:nucl-ex/0607029](#), [doi:10.1103/PhysRevLett.97.262002](#).
- [17] M. Mazouz, et al., Deeply virtual compton scattering off the neutron, *Phys. Rev. Lett.* 99 (2007) 242501. [arXiv:0709.0450](#), [doi:10.1103/PhysRevLett.99.242501](#).
- [18] S. Stepanyan, et al., Observation of exclusive deeply virtual Compton scattering in polarized electron beam asymmetry measurements, *Phys. Rev. Lett.* 87 (2001) 182002. [arXiv:hep-ex/0107043](#), [doi:10.1103/PhysRevLett.87.182002](#).
- [19] S. Chen, et al., Measurement of deeply virtual compton scattering with a polarized proton target, *Phys. Rev. Lett.* 97 (2006) 072002. [arXiv:hep-ex/0605012](#), [doi:10.1103/PhysRevLett.97.072002](#).
- [20] F. X. Girod, et al., Measurement of Deeply virtual Compton scattering beam-spin asymmetries, *Phys. Rev. Lett.* 100 (2008) 162002. [arXiv:0711.4805](#), [doi:10.1103/PhysRevLett.100.162002](#).
- [21] J. Breitweg, et al., Exclusive electroproduction of ρ^0 and J/ψ mesons at HERA, *Eur. Phys. J. C* 6 (1999) 603–627. [arXiv:hep-ex/9808020](#), [doi:10.1007/s100529901051](#).
- [22] S. Chekanov, et al., Measurement of deeply virtual Compton scattering at HERA, *Phys. Lett. B* 573 (2003) 46–62. [arXiv:hep-ex/0305028](#), [doi:10.1016/j.physletb.2003.08.048](#).
- [23] C. Adloff, et al., Measurement of deeply virtual Compton scattering at HERA, *Phys. Lett. B* 517 (2001) 47–58. [arXiv:hep-ex/0107005](#), [doi:10.1016/S0370-2693\(01\)00939-X](#).
- [24] A. Aktas, et al., Measurement of deeply virtual compton scattering at HERA, *Eur. Phys. J. C* 44 (2005) 1–11. [arXiv:hep-ex/0505061](#), [doi:10.1140/epjc/s2005-02345-3](#).
- [25] A. Airapetian, et al., Measurement of the beam spin azimuthal asymmetry associated with deeply virtual Compton scattering, *Phys. Rev. Lett.* 87 (2001) 182001. [arXiv:hep-ex/0106068](#), [doi:10.1103/PhysRevLett.87.182001](#).
- [26] A. Airapetian, et al., The Beam-charge azimuthal asymmetry and deeply virtual compton scattering, *Phys. Rev. D* 75 (2007) 011103. [arXiv:hep-ex/0605108](#), [doi:10.1103/PhysRevD.75.011103](#).
- [27] A. Airapetian, et al., Measurement of Azimuthal Asymmetries With Respect To Both Beam Charge and Transverse Target Polarization in Exclusive Electroproduction of Real Photons, *JHEP* 06 (2008) 066. [arXiv:0802.2499](#), [doi:10.1088/1126-6708/2008/06/066](#).
- [28] N. d’Hose, E. Burtin, P. A. M. Guichon, J. Marroncle, Feasibility study of deeply virtual Compton scattering using COMPASS at CERN, *Eur. Phys. J. A* 19S1 (2004) 47–53. [doi:10.1140/epjad/s2004-03-008-x](#).
- [29] A. Accardi, et al., Electron Ion Collider: The Next QCD Frontier: Understanding the glue that binds us all, *Eur. Phys. J. A* 52 (9) (2016) 268. [arXiv:1212.1701](#), [doi:10.1140/epja/i2016-16268-9](#).
- [30] R. Abdul Khalek, et al., Science Requirements and Detector Concepts for the Electron-Ion Collider: EIC Yellow Report, *Nucl. Phys. A* 1026 (2022) 122447. [arXiv:2103.05419](#), [doi:10.1016/j.nuclphysa.2022.122447](#).
- [31] D. P. Anderle, et al., Electron-ion collider in China, *Front. Phys. (Beijing)* 16 (6) (2021) 64701. [arXiv:2102.09222](#), [doi:10.1007/s11467-021-1062-0](#).
- [32] R. Abdul Khalek, et al., Snowmass 2021 White Paper: Electron Ion Collider for High Energy Physics [arXiv:2203.13199](#).
- [33] R. Abir, et al., The case for an EIC Theory Alliance: Theoretical Challenges of the EIC [arXiv:2305.14572](#).
- [34] S. Amoroso, et al., Snowmass 2021 Whitepaper: Proton Structure at the Precision Frontier, *Acta Phys. Polon. B* 53 (12) (2022) 12–A1. [arXiv:2203.13923](#), [doi:10.5506/APhysPolB.53.12-A1](#).
- [35] M. Hentschinski, et al., White Paper on Forward Physics, BFKL, Saturation Physics and Diffraction, *Acta Phys. Polon. B* 54 (3) (2023) 3–A2. [arXiv:2203.08129](#), [doi:10.5506/APhysPolB.54.3-A2](#).

- [36] J. L. Abelleira Fernandez, et al., A Large Hadron Electron Collider at CERN: Report on the Physics and Design Concepts for Machine and Detector, *J. Phys. G* 39 (2012) 075001. [arXiv:1206.2913](#), [doi:10.1088/0954-3899/39/7/075001](#).
- [37] P. Agostini, et al., The Large Hadron–Electron Collider at the HL-LHC, *J. Phys. G* 48 (11) (2021) 110501. [arXiv:2007.14491](#), [doi:10.1088/1361-6471/abf3ba](#).
- [38] J. Dudek, et al., Physics Opportunities with the 12 GeV Upgrade at Jefferson Lab, *Eur. Phys. J. A* 48 (2012) 187. [arXiv:1208.1244](#), [doi:10.1140/epja/i2012-12187-1](#).
- [39] V. D. Burkert, Jefferson Lab at 12 GeV: The Science Program, *Ann. Rev. Nucl. Part. Sci.* 68 (2018) 405–428. [doi:10.1146/annurev-nucl-101917-021129](#).
- [40] A. Accardi, et al., Strong interaction physics at the luminosity frontier with 22 GeV electrons at Jefferson Lab, *Eur. Phys. J. A* 60 (9) (2024) 173. [arXiv:2306.09360](#), [doi:10.1140/epja/s10050-024-01282-x](#).
- [41] M. Burkardt, Impact parameter dependent parton distributions and off forward parton distributions for $zeta \rightarrow 0$, *Phys. Rev. D* 62 (2000) 071503, [Erratum: *Phys. Rev. D* 66, 119903 (2002)]. [arXiv:hep-ph/0005108](#), [doi:10.1103/PhysRevD.62.071503](#).
- [42] M. Burkardt, Impact parameter space interpretation for generalized parton distributions, *Int. J. Mod. Phys. A* 18 (2003) 173–208. [arXiv:hep-ph/0207047](#), [doi:10.1142/S0217751X03012370](#).
- [43] J. P. Ralston, B. Pire, Femtophotography of protons to nuclei with deeply virtual Compton scattering, *Phys. Rev. D* 66 (2002) 111501. [arXiv:hep-ph/0110075](#), [doi:10.1103/PhysRevD.66.111501](#).
- [44] S. J. Brodsky, D. Chakrabarti, A. Harindranath, A. Mukherjee, J. P. Vary, Hadron optics: Diffraction patterns in deeply virtual Compton scattering, *Phys. Lett. B* 641 (2006) 440–446. [arXiv:hep-ph/0604262](#), [doi:10.1016/j.physletb.2006.08.061](#).
- [45] S. J. Brodsky, D. Chakrabarti, A. Harindranath, A. Mukherjee, J. P. Vary, Hadron optics in three-dimensional invariant coordinate space from deeply virtual Compton scattering, *Phys. Rev. D* 75 (2007) 014003. [arXiv:hep-ph/0611159](#), [doi:10.1103/PhysRevD.75.014003](#).
- [46] D. Chakrabarti, R. Manohar, A. Mukherjee, Chiral odd GPDs in transverse and longitudinal impact parameter spaces, *Phys. Rev. D* 79 (2009) 034006. [arXiv:0811.0521](#), [doi:10.1103/PhysRevD.79.034006](#).
- [47] R. Manohar, A. Mukherjee, D. Chakrabarti, Generalized Parton Distributions for the Proton in Position Space : Non-Zero Skewness, *Phys. Rev. D* 83 (2011) 014004. [arXiv:1012.2627](#), [doi:10.1103/PhysRevD.83.014004](#).
- [48] N. Kumar, H. Dahiya, Generalized Parton Distributions of proton for nonzero skewness in transverse and longitudinal position spaces, *Int. J. Mod. Phys. A* 30 (02) (2015) 1550010. [arXiv:1501.04745](#), [doi:10.1142/S0217751X15500104](#).
- [49] C. Mondal, D. Chakrabarti, Generalized parton distributions and transverse densities in a light-front quark–diquark model for the nucleons, *Eur. Phys. J. C* 75 (6) (2015) 261. [arXiv:1501.05489](#), [doi:10.1140/epjc/s10052-015-3486-6](#).
- [50] D. Chakrabarti, C. Mondal, Chiral-odd generalized parton distributions for proton in a light-front quark–diquark model, *Phys. Rev. D* 92 (7) (2015) 074012. [arXiv:1509.00598](#), [doi:10.1103/PhysRevD.92.074012](#).
- [51] C. Mondal, Helicity-dependent generalized parton distributions for nonzero skewness, *Eur. Phys. J. C* 77 (9) (2017) 640. [arXiv:1709.06877](#), [doi:10.1140/epjc/s10052-017-5203-0](#).
- [52] B. Pasquini, M. Pincetti, S. Boffi, Chiral-odd generalized parton distributions in constituent quark models, *Phys. Rev. D* 72 (2005) 094029. [arXiv:hep-ph/0510376](#), [doi:10.1103/PhysRevD.72.094029](#).
- [53] B. Pasquini, S. Boffi, Virtual meson cloud of the nucleon and generalized parton distributions, *Phys. Rev. D* 73 (2006) 094001. [arXiv:hep-ph/0601177](#), [doi:10.1103/PhysRevD.73.094001](#).
- [54] S. Meissner, A. Metz, M. Schlegel, Generalized parton correlation functions for a spin-1/2 hadron, *JHEP* 08 (2009) 056. [arXiv:0906.5323](#), [doi:10.1088/1126-6708/2009/08/056](#).
- [55] S. Boffi, B. Pasquini, M. Traini, Linking generalized parton distributions to constituent quark models, *Nucl. Phys. B* 649 (2003) 243–262. [arXiv:hep-ph/0207340](#), [doi:10.1016/S0550-3213\(02\)01016-7](#).
- [56] S. Scopetta, V. Vento, Generalized parton distributions and composite constituent quarks, *Phys. Rev. D* 69 (2004) 094004. [arXiv:hep-ph/0307150](#), [doi:10.1103/PhysRevD.69.094004](#).
- [57] H.-M. Choi, C.-R. Ji, L. S. Kisslinger, Skewed quark distribution of the pion in the light front quark model, *Phys. Rev. D* 64 (2001) 093006. [arXiv:hep-ph/0104117](#), [doi:10.1103/PhysRevD.64.093006](#).
- [58] H.-M. Choi, C.-R. Ji, L. S. Kisslinger, Continuity of skewed parton distributions for the pion virtual Compton scattering, *Phys. Rev. D* 66 (2002) 053011. [arXiv:hep-ph/0204321](#), [doi:10.1103/PhysRevD.66.053011](#).
- [59] S. Kaur, S. Xu, C. Mondal, X. Zhao, J. P. Vary, Spatial imaging of proton via leading-twist nonskewed GPDs with basis light-front quantization, *Phys. Rev. D* 109 (1) (2024) 014015. [arXiv:2307.09869](#), [doi:10.1103/PhysRevD.109.014015](#).
- [60] X. Ji, Parton Physics on a Euclidean Lattice, *Phys. Rev. Lett.* 110 (2013) 262002. [arXiv:1305.1539](#), [doi:10.1103/PhysRevLett.110.262002](#).
- [61] X. Ji, Y.-S. Liu, Y. Liu, J.-H. Zhang, Y. Zhao, Large-momentum effective theory, *Rev. Mod. Phys.* 93 (3) (2021) 035005. [arXiv:2004.03543](#), [doi:10.1103/RevModPhys.93.035005](#).
- [62] H.-W. Lin, Nucleon helicity generalized parton distribution at physical pion mass from lattice QCD, *Phys. Lett. B* 824 (2022) 136821. [arXiv:2112.07519](#), [doi:10.1016/j.physletb.2021.136821](#).
- [63] H.-W. Lin, Nucleon Tomography and Generalized Parton Distribution at Physical Pion Mass from Lattice QCD, *Phys. Rev. Lett.* 127 (18) (2021) 182001. [arXiv:2008.12474](#), [doi:10.1103/PhysRevLett.127.182001](#).
- [64] S. Bhattacharya, K. Cichy, M. Constantinou, J. Dodson, X. Gao, A. Metz, S. Mukherjee, A. Scapellato, F. Steffens, Y. Zhao, Generalized parton distributions from lattice QCD with asymmetric momentum transfer: Unpolarized quarks, *Phys. Rev. D* 106 (11) (2022) 114512. [arXiv:2209.05373](#), [doi:10.1103/PhysRevD.106.114512](#).
- [65] C. Alexandrou, K. Cichy, M. Constantinou, K. Hadjiyianakou, K. Jansen, A. Scapellato, F. Steffens, Transversity GPDs of the proton from lattice QCD, *Phys. Rev. D* 105 (3) (2022) 034501. [arXiv:2108.10789](#), [doi:10.1103/PhysRevD.105.034501](#).
- [66] C. Alexandrou, et al., Moments of the nucleon transverse quark spin densities using lattice QCD, *Phys. Rev. D* 107 (5) (2023) 054504. [arXiv:2202.09871](#), [doi:10.1103/PhysRevD.107.054504](#).
- [67] Y. Guo, X. Ji, K. Shiells, Generalized parton distributions through universal moment parameterization: zero skewness case, *JHEP* 09 (2022) 215. [arXiv:2207.05768](#), [doi:10.1007/JHEP09\(2022\)215](#).
- [68] C. Alexandrou, K. Cichy, M. Constantinou, K. Hadjiyianakou, K. Jansen, A. Scapellato, F. Steffens, Unpolarized and helicity generalized parton distributions of the proton within lattice QCD, *Phys. Rev. Lett.* 125 (26) (2020) 262001. [arXiv:2008.10573](#), [doi:10.1103/PhysRevLett.125.262001](#).
- [69] M. Gockeler, P. Hagler, R. Horsley, D. Pleiter, P. E. L. Rakow, A. Schafer, G. Schierholz, J. M. Zanotti, Quark helicity flip generalized parton distributions from two-flavor lattice QCD, *Phys. Lett. B* 627 (2005) 113–123. [arXiv:hep-lat/0507001](#), [doi:10.1016/j.physletb.2005.09.002](#).
- [70] M. Gockeler, P. Hägler, R. Horsley, Y. Nakamura, D. Pleiter, P. E. L. Rakow, A. Schäfer, G. Schierholz, H. Stüben, J. M. Zanotti, Transverse spin structure of the nucleon from lattice QCD simulations, *Phys. Rev. Lett.* 98 (2007) 222001. [arXiv:hep-lat/0612032](#), [doi:10.1103/PhysRevLett.98.222001](#).

- [71] C. Alexandrou, et al., Moments of nucleon generalized parton distributions from lattice QCD simulations at physical pion mass, *Phys. Rev. D* 101 (3) (2020) 034519. [arXiv:1908.10706](#), [doi:10.1103/PhysRevD.101.034519](#).
- [72] A. Hannaford-Gunn, K. U. Can, J. A. Crawford, R. Horsley, P. E. L. Rakow, G. Schierholz, H. Stüben, R. D. Young, J. M. Zanotti, Reconstructing generalized parton distributions from the lattice off-forward Compton amplitude, *Phys. Rev. D* 110 (1) (2024) 014509. [arXiv:2405.06256](#), [doi:10.1103/PhysRevD.110.014509](#).
- [73] C. Tan, Z. Lu, Gluon generalized parton distributions and angular momentum in a light-cone spectator model, *Phys. Rev. D* 108 (5) (2023) 054038. [arXiv:2301.09081](#), [doi:10.1103/PhysRevD.108.054038](#).
- [74] D. Chakrabarti, P. Choudhary, B. Gurjar, T. Maji, C. Mondal, A. Mukherjee, Gluon generalized parton distributions of the proton at nonzero skewness, *Phys. Rev. D* 109 (11) (2024) 114040. [arXiv:2402.16503](#), [doi:10.1103/PhysRevD.109.114040](#).
- [75] D. Chakrabarti, P. Choudhary, B. Gurjar, R. Kishore, T. Maji, C. Mondal, A. Mukherjee, Gluon distributions in the proton in a light-front spectator model, *Phys. Rev. D* 108 (1) (2023) 014009. [arXiv:2304.09908](#), [doi:10.1103/PhysRevD.108.014009](#).
- [76] B. Lin, S. Nair, S. Xu, Z. Hu, C. Mondal, X. Zhao, J. P. Vary, Generalized parton distributions of gluon in proton: A light-front quantization approach, *Phys. Lett. B* 847 (2023) 138305. [arXiv:2308.08275](#), [doi:10.1016/j.physletb.2023.138305](#).
- [77] B. Lin, S. Nair, C. Mondal, S. Xu, Z. Hu, P. Zhang, X. Zhao, J. P. Vary, Chiral-odd gluon generalized parton distributions in the proton: A light-front quantization approach, *Phys. Lett. B* 860 (2025) 139153. [arXiv:2408.09988](#), [doi:10.1016/j.physletb.2024.139153](#).
- [78] B. Gurjar, C. Mondal, D. Chakrabarti, Polarized gluon distribution in the proton from holographic light-front QCD, *Phys. Rev. D* 107 (5) (2023) 054013. [arXiv:2209.14285](#), [doi:10.1103/PhysRevD.107.054013](#).
- [79] G. F. de Téramond, H. G. Dosch, T. Liu, R. S. Sufian, S. J. Brodsky, A. Deur, Gluon matter distribution in the proton and pion from extended holographic light-front QCD, *Phys. Rev. D* 104 (11) (2021) 114005. [arXiv:2107.01231](#), [doi:10.1103/PhysRevD.104.114005](#).
- [80] K. A. Mamo, I. Zahed, Parametrization of Generalized Parton Distributions from t-Channel String Exchange in AdS Spaces, *Phys. Rev. Lett.* 133 (24) (2024) 241901. [arXiv:2411.04162](#), [doi:10.1103/PhysRevLett.133.241901](#).
- [81] K. A. Mamo, I. Zahed, String-based parametrization of nucleon GPDs at any skewness: A comparison to lattice QCD, *Phys. Rev. D* 110 (11) (2024) 114016. [arXiv:2404.13245](#), [doi:10.1103/PhysRevD.110.114016](#).
- [82] J. P. Vary, H. Honkanen, J. Li, P. Maris, S. J. Brodsky, A. Harindranath, G. F. de Téramond, P. Sternberg, E. G. Ng, C. Yang, Hamiltonian light-front field theory in a basis function approach, *Phys. Rev. C* 81 (2010) 035205. [arXiv:0905.1411](#), [doi:10.1103/PhysRevC.81.035205](#).
- [83] X. Zhao, H. Honkanen, P. Maris, J. P. Vary, S. J. Brodsky, Electron $g-2$ in Light-Front Quantization, *Phys. Lett. B* 737 (2014) 65–69. [arXiv:1402.4195](#), [doi:10.1016/j.physletb.2014.08.020](#).
- [84] Y. Li, P. Maris, X. Zhao, J. P. Vary, Heavy Quarkonium in a Holographic Basis, *Phys. Lett. B* 758 (2016) 118–124. [arXiv:1509.07212](#), [doi:10.1016/j.physletb.2016.04.065](#).
- [85] S. Nair, C. Mondal, X. Zhao, A. Mukherjee, J. P. Vary, Basis light-front quantization approach to photon, *Phys. Lett. B* 827 (2022) 137005. [arXiv:2201.12770](#), [doi:10.1016/j.physletb.2022.137005](#).
- [86] J. Lan, C. Mondal, S. Jia, X. Zhao, J. P. Vary, Parton Distribution Functions from a Light Front Hamiltonian and QCD Evolution for Light Mesons, *Phys. Rev. Lett.* 122 (17) (2019) 172001. [arXiv:1901.11430](#), [doi:10.1103/PhysRevLett.122.172001](#).
- [87] C. Mondal, S. Xu, J. Lan, X. Zhao, Y. Li, D. Chakrabarti, J. P. Vary, Proton structure from a light-front Hamiltonian, *Phys. Rev. D* 102 (1) (2020) 016008. [arXiv:1911.10913](#), [doi:10.1103/PhysRevD.102.016008](#).
- [88] S. Xu, C. Mondal, J. Lan, X. Zhao, Y. Li, J. P. Vary, Nucleon structure from basis light-front quantization, *Phys. Rev. D* 104 (9) (2021) 094036. [arXiv:2108.03909](#), [doi:10.1103/PhysRevD.104.094036](#).
- [89] J. Lan, K. Fu, C. Mondal, X. Zhao, J. P. Vary, Light mesons with one dynamical gluon on the light front, *Phys. Lett. B* 825 (2022) 136890. [arXiv:2106.04954](#), [doi:10.1016/j.physletb.2022.136890](#).
- [90] S. Xu, C. Mondal, X. Zhao, Y. Li, J. P. Vary, Quark and gluon spin and orbital angular momentum in the proton, *Phys. Rev. D* 108 (9) (2023) 094002. [doi:10.1103/PhysRevD.108.094002](#).
- [91] H. Yu, Z. Hu, S. Xu, C. Mondal, X. Zhao, J. P. Vary, Transverse-momentum-dependent gluon distributions of proton within basis light-front quantization, *Phys. Lett. B* 855 (2024) 138831. [arXiv:2403.06125](#), [doi:10.1016/j.physletb.2024.138831](#).
- [92] Z. Zhu, S. Xu, J. Wu, H. Yu, Z. Hu, J. Lan, C. Mondal, X. Zhao, J. P. Vary, Transverse structure of the proton beyond leading twist: A light-front Hamiltonian approach, *Phys. Lett. B* 855 (2024) 138829. [arXiv:2404.13720](#), [doi:10.1016/j.physletb.2024.138829](#).
- [93] S. J. Brodsky, H.-C. Pauli, S. S. Pinsky, Quantum chromodynamics and other field theories on the light cone, *Phys. Rept.* 301 (1998) 299–486. [arXiv:hep-ph/9705477](#), [doi:10.1016/S0370-1573\(97\)00089-6](#).
- [94] R. J. Perry, A. Harindranath, K. G. Wilson, Light front Tamm-Dancoff field theory, *Phys. Rev. Lett.* 65 (1990) 2959–2962. [doi:10.1103/PhysRevLett.65.2959](#).
- [95] V. A. Karmanov, J. F. Mathiot, A. V. Smirnov, Systematic renormalization scheme in light-front dynamics with Fock space truncation, *Phys. Rev. D* 77 (2008) 085028. [arXiv:0801.4507](#), [doi:10.1103/PhysRevD.77.085028](#).
- [96] A. Kurganov, et al., Method of Experimental Alignment of Detectors in the DPS-NICA Project, *Phys. Part. Nucl. Lett.* 21 (2) (2024) 178–185. [doi:10.1134/S1547477124020080](#).
- [97] S. D. Glazek, R. J. Perry, Special example of relativistic Hamiltonian field theory, *Phys. Rev. D* 45 (1992) 3740–3754. [doi:10.1103/PhysRevD.45.3740](#).
- [98] M. Burkardt, Dynamical vertex mass generation and chiral symmetry breaking on the light front, *Phys. Rev. D* 58 (1998) 096015. [arXiv:hep-th/9805088](#), [doi:10.1103/PhysRevD.58.096015](#).
- [99] M. Diehl, Generalized parton distributions, *Phys. Rept.* 388 (2003) 41–277. [arXiv:hep-ph/0307382](#), [doi:10.1016/j.physrep.2003.08.002](#).
- [100] Y. Liu, S. Xu, C. Mondal, Z. Hu, X. Zhao, J. P. Vary, Skewed generalized parton distributions of proton from basis light-front quantization, *Phys. Lett. B* 855 (2024) 138809. [arXiv:2403.05922](#), [doi:10.1016/j.physletb.2024.138809](#).
- [101] X.-D. Ji, W. Melnitchouk, X. Song, A Study of off forward parton distributions, *Phys. Rev. D* 56 (1997) 5511–5523. [arXiv:hep-ph/9702379](#), [doi:10.1103/PhysRevD.56.5511](#).
- [102] S. Boffi, B. Pasquini, M. Traini, Helicity dependent generalized parton distributions in constituent quark models, *Nucl. Phys. B* 680 (2004) 147–163. [arXiv:hep-ph/0311016](#), [doi:10.1016/j.nuclphysb.2003.12.037](#).
- [103] A. Freese, I. C. Cloët, Quark spin and orbital angular momentum from proton generalized parton distributions, *Phys. Rev. C* 103 (4) (2021) 045204. [arXiv:2005.10286](#), [doi:10.1103/PhysRevC.103.045204](#).
- [104] N. Kaur, N. Kumar, C. Mondal, H. Dahiya, Generalized Parton Distributions of Pion for Non-Zero Skewness in AdS/QCD, *Nucl. Phys. B* 934 (2018) 80–95. [arXiv:1807.01076](#), [doi:10.1016/j.nuclphysb.2018.07.003](#).
- [105] S. Meissner, A. Metz, K. Goeke, Relations between generalized and transverse momentum dependent parton distributions, *Phys. Rev. D* 76 (2007) 034002. [arXiv:hep-ph/0703176](#),

[doi:10.1103/PhysRevD.76.034002](https://doi.org/10.1103/PhysRevD.76.034002).

- [106] M. Diehl, P. Hagler, Spin densities in the transverse plane and generalized transversity distributions, *Eur. Phys. J. C* 44 (2005) 87–101. [arXiv:hep-ph/0504175](https://arxiv.org/abs/hep-ph/0504175), [doi:10.1140/epjc/s2005-02342-6](https://doi.org/10.1140/epjc/s2005-02342-6).
- [107] M. Burkardt, Transverse deformation of parton distributions and transversity decomposition of angular momentum, *Phys. Rev. D* 72 (2005) 094020. [arXiv:hep-ph/0505189](https://arxiv.org/abs/hep-ph/0505189), [doi:10.1103/PhysRevD.72.094020](https://doi.org/10.1103/PhysRevD.72.094020).
- [108] M. Diehl, Generalized parton distributions in impact parameter space, *Eur. Phys. J. C* 25 (2002) 223–232, [Erratum: *Eur.Phys.J.C* 31, 277–278 (2003)]. [arXiv:hep-ph/0205208](https://arxiv.org/abs/hep-ph/0205208), [doi:10.1007/s10052-002-1016-9](https://doi.org/10.1007/s10052-002-1016-9).
- [109] S. J. Brodsky, M. Diehl, D. S. Hwang, Light cone wave function representation of deeply virtual Compton scattering, *Nucl. Phys. B* 596 (2001) 99–124. [arXiv:hep-ph/0009254](https://arxiv.org/abs/hep-ph/0009254), [doi:10.1016/S0550-3213\(00\)00695-7](https://doi.org/10.1016/S0550-3213(00)00695-7).
- [110] G. A. Miller, S. J. Brodsky, Frame-independent spatial coordinate \tilde{z} : Implications for light-front wave functions, deep inelastic scattering, light-front holography, and lattice QCD calculations, *Phys. Rev. C* 102 (2) (2020) 022201. [arXiv:1912.08911](https://arxiv.org/abs/1912.08911), [doi:10.1103/PhysRevC.102.022201](https://doi.org/10.1103/PhysRevC.102.022201).
- [111] T. Maji, C. Mondal, D. Kang, Leading twist GTMDs at nonzero skewness and Wigner distributions in boost-invariant longitudinal position space, *Phys. Rev. D* 105 (7) (2022) 074024. [arXiv:2202.08635](https://arxiv.org/abs/2202.08635), [doi:10.1103/PhysRevD.105.074024](https://doi.org/10.1103/PhysRevD.105.074024).
- [112] V. K. Ojha, S. Jana, T. Maji, Quark generalized TMDs at skewness and Wigner distributions in boost invariant longitudinal space, *Phys. Rev. D* 107 (7) (2023) 074040. [arXiv:2211.02959](https://arxiv.org/abs/2211.02959), [doi:10.1103/PhysRevD.107.074040](https://doi.org/10.1103/PhysRevD.107.074040).
- [113] C. M. Weller, G. A. Miller, Confinement in two-dimensional QCD and the infinitely long pion, *Phys. Rev. D* 105 (3) (2022) 036009. [arXiv:2111.03194](https://arxiv.org/abs/2111.03194), [doi:10.1103/PhysRevD.105.036009](https://doi.org/10.1103/PhysRevD.105.036009).
- [114] Z. Zhang, Z. Hu, S. Xu, C. Mondal, X. Zhao, J. P. Vary, Twist-3 generalized parton distribution for the proton from basis light-front quantization, *Phys. Rev. D* 109 (3) (2024) 034031. [arXiv:2312.00667](https://arxiv.org/abs/2312.00667), [doi:10.1103/PhysRevD.109.034031](https://doi.org/10.1103/PhysRevD.109.034031).